Journal of Power Sources 189 (2009) 471–475

Contents lists available at ScienceDirect

Journal of Power Sources

journal homepage: www.elsevier.com/locate/jpowsour

Short communication

Cathode having high rate performance for a secondary Li-ion cell surface-modified by aluminum oxide nanoparticles

Toyoki Okumura[a], Tomokazu Fukutsuka[a], Yoshiharu Uchimoto[a,*], Koji Amezawa[b], Shota Kobayashi[c]

[a] Graduate School of Human and Environmental Studies, Kyoto University, Yoshida-nihonmatsu-cho, Sakyo-ku, Kyoto 06-8501, Japan
[b] Graduate School of Environmental Studies, Tohoku University, 6-6-01 Aoba, Aramaki, Aoba-ku, Sendai 980-8579, Japan
[c] Department of Applied Chemistry, Tokyo Institute of Technology, Tokyo 152-8552, Japan

ARTICLE INFO

Article history:
Received 28 July 2008
Received in revised form 9 September 2008
Accepted 11 December 2008
Available online 24 December 2008

Keywords:
High power density
Surface modification
$LiMn_2O_4$
Electrode/electrolyte interface

ABSTRACT

In order to enhance the electrochemical properties, the spinel $LiMn_2O_4$ electrode surface was modified with amorphous Al_2O_3 nanoparticle as heterogeneous phase. $LiMn_2O_4$ was in preparation based on a conventional solid-state reaction. The $LiMn_2O_4$ procedure was soaked in aluminum tri 2-propoxide solution. The $LiMn_2O_4$ whose surface was modified by aluminum oxide was obtained through the heat treatment at 400 °C for 4 h. The Al_2O_3-modified $LiMn_2O_4$ electrode exhibits a capacity higher than that of the unmodified $LiMn_2O_4$ electrode. On the other hand, no variation was shown with open circuit potential and apparent chemical diffusion coefficient of Li ion for $LiMn_2O_4$ before and after the surface modification. The charge-transfer resistance of Al_2O_3-modified $LiMn_2O_4$ decreased significantly in comparison with the unmodified $LiMn_2O_4$. The improved charge-transfer kinetics was largely attributed to Al_2O_3 which plays an important role of increasing the chemical potential at the electrode/electrolyte interface.

1. Introduction

Li-ion secondary batteries have widely been utilized as consumers' electronic devices such as cellular phones, personal computers, etc. because of their highness in energy density [1]. Consideration is also being taken with the batteries to apply them for a measure for transportation in a style of a hybrid electric vehicle (HEV). Their marketability is enormous enough in comparison with the other methods for the currently used application. Especially to be utilized for HEV application, high-rate performance is required with the batteries. With conventional Li-ion batteries, cycle life and performance are liable to be reduced by high-rate discharging and charging. Therefore it is required that Li-ion batteries should be operated without being degraded by high power density.

In electrochemical cathodic reaction in the Li-ion secondary batteries, some reaction steps are included in a style such as of diffusion or transfer of Li-ion in the electrolyte bulk, adsorption and absorption of Li-ions on the electrode surface, charge-transfer reaction at the electrolyte/electrode interface, and diffusion of Li-ions in the electrode bulk [2]. The kinetics of the electrochemical reactions at the electrolyte/electrode interface depends on electrochemical potential of lithium ions. The promotion of the transfer can be achieved by introducing heterogeneous, second phase interacting with lithium ions or counter anions of lithium salt in the electrolyte.

Previously some research groups have released their reports for heterogeneous doping in connection with the second phase directed towards the solid inorganic and/or polymer electrolyte [3–7]. Success was gained with the heterogeneous doping in enhancing the moderate ionic conductivity [3]. The conductivity enhancement in heterogeneously doped halide can be explained quantitatively by the ideal space charge effect [4]. Al_2O_3, $SrTiO_3$, CeO_2, SiO_2, and ZrO_2, which are prominent oxides as materials, induce such a space charge layer [5,6]. Liang [7] has reported that excessively high anomalousness was noticed with the electrical properties of the two-phase system $LiI–Al_2O_3$ in comparison with those of the pure phases. Such solid electrolyte systems are widely known as composite electrolytes or heterogeneous electrolytes. Recently, Scrosati and co-workers [8] have released a report stating to the effect that addition of nanoparticle fillers, such as Al_2O_3 or TiO_2, to simple PEO compounds brings about several-times increase in the conductivity at 60–80 °C. Therefore it is expected that it will be possible for the interaction of the aluminum oxide and lithium salt at the electrode/electrolyte interface to promote the kinetics.

This paper describes that enhancement can be noticed with the electrochemical potential of the lithium ion at interface, using surface treatment of $LiMn_2O_4$. The said substance having porosity of aluminum oxide nanoparticle is an alternative material to substitute layered $LiCoO_2$ cathode for 4 V-lithium rechargeable batteries.

* Corresponding author. Tel.: +81 75 753 2924; fax: +81 75 753 2924.
E-mail address: uchimoto@chem.mbox.media.kyoto-u.ac.jp (Y. Uchimoto).

0378-7753/$ – see front matter © 2008 Elsevier B.V. All rights reserved.
doi:10.1016/j.jpowsour.2008.12.043

Many research groups have made reports concerning the surface modification of cathode with a view to multiplying rechargeable properties or thermal stability [9]. However to our knowledge, this paper of ours showed for the first time enhancement of electrochemical reaction kinetics by introducing of a heterogeneous phase to the surface of the cathode.

2. Experimental

$LiMn_2O_4$ was in preparation based on a conventional solid-state reaction brought about from a stoichiometric mixture of Li_2CO_3 (99.9% Soekawa chemicals) and Mn_2O_3 (99.9% Kojundo chemicals) (1:1 mol. ratio) at 750 °C for 72 h exposed to air. The $LiMn_2O_4$ resulted from the above preparation procedure was soaked in 10 mmol dm^{-3} 2-propanol containing aluminum tri 2-propoxide (99% Soekawa chemicals) for 3 h to be finally filtered. The $LiMn_2O_4$ whose surface was modified by aluminum oxide was obtained through the heat treatment at 400 °C for 4 h.

The phase identification of the prepared samples was performed by X-ray diffractometry (XRD), using a Rigaku RINT2500 V with Cu Kα radiation. Al K-edged X-ray absorption near edge structure (XANES) and Mn *L*-edge XANES were measured at BL-IA and BL-8BI beamline in UVSOR (Okazaki, Japan) with a ring energy of 750 MeV in a mode of total electron yield at room temperature. The morphology was examined and measurement of particle size distribution was made with the aid of a scanning electron microscope, SEM (JSM-5310LV) and Beckman Coulter LS230.

Samples were examined with their electrochemical characteristics, using a three-electrode electrochemical cell. The working electrodes were taken up for preparation by mixing the specimen powder (80 wt.%) with carbon black (10 wt.%) and polyvinylidine fluoride (10 wt.%). Lithium foils were employed as counter and reference electrodes. All of which had constant weight and surface area. The electrolyte was 0.1–1 mol dm^{-3} solution of $LiPF_6$ in 1:1 (vol. ratio) EC/DMC. EIS was performed, using a frequency response analyzer (Solatron 1255B) and potentio/galvanostat (1287) driven by the Corrware for Windows software (Scribner Associates) at seven different temperatures in a range of 5–35 °C. The frequency range from 100 kHz to 5 mHz was covered by the impedance spectra with a.c. amplitude 10 mV. Before performing EIS measurements, the potential was changed to 4.0 V and held at the given potential. Then, it is thought that the lithium concentration in the $LiMn_2O_4$ bulk is in the equilibrium state. Analysis was made with the measured impedance data, employing a complex non-linear least squares fitting program (Z-plot for Windows, Scribner Associates). All the electrochemical experiments were conducted in a glove box filled with a purified argon gas.

3. Results and discussion

Fig. 1 shows unmodified and Al_2O_3-modified $LiMn_2O_4$ samples. XRD pattern of $LiMn_2O_4$ synthesized by the solid-state reaction was a well-defined spinel single phase belonging to the space group *Fd*-3*m*. Spinel structure was continuously maintained despite absence of an impurity phase after the surface modification. With lattice parameters of $LiMn_2O_4$, no change has been effected upon modification by Al_2O_3. This suggests that no bulk structure was affected by surface modification. None of XRD patterns showed any peaks corresponding to Al_2O_3. In order to investigate changes in Mn valence before and after the surface modification, Mn *L*-edge XANES measurement was performed. The Mn *L*-edge XANES spectra show no detectable change before and after the surface modification, indicating that the aluminum on the particle surface prevents solid solution with $LiMn_2O_4$ from being formed. No apparent changes were noticed in the surface morphology before and after the surface modification from SEM micrograph. From the results of the particle size distribution measurements, it is explained that there was no difference in the size distribution between the Al_2O_3 modified and the unmodified $LiMn_2O_4$ (the average particle diameter is 2 μm). This is because the aluminum oxides attached to the particle surface are extremely fine (the amount of the modified compound applied corresponded to approximately 0.3% by weight in unmodified $LiMn_2O_4$ (inductivity coupled plasma)).

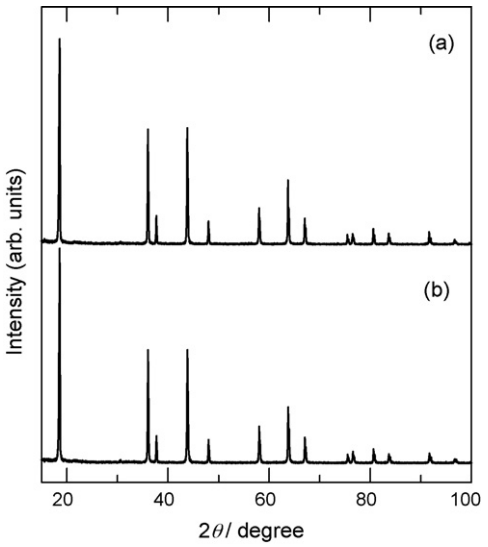

Fig. 1. XRD patterns of (a) unmodified and (b) Al_2O_3-modified $LiMn_2O_4$ samples.

To obtain the information concerning the component of the modified compounds on the $LiMn_2O_4$ particle surface, Al *K*-edge XANES measurements were performed. Fig. 2 shows Al K-edge XANES spectra of Al_2O_3-modified $LiMn_2O_4$ and amorphous Al_2O_3. The shape of Al *K*-edge XANES spectrum is in coincidence with that of amorphous Al_2O_3. Thus Al_2O_3 existing on the surface of $LiMn_2O_4$ particle is found in the amorphous materials [10]. To analyze the concentration profile drawn into the particle, the depth of Al_2O_3 modified as $LiMn_2O_4$ was obtained by Auger electron spectroscopy. Aluminum atoms of the modified $LiMn_2O_4$ were distributed exclusively at the particle surface in a range within 20 nm. As shown in Fig. 3, TEM observation reveals very clearly that $LiMn_2O_4$ particles were covered by the amorphous Al_2O_3 nanoparticles whose diameter is 10–20 nm.

The Al_2O_3-modified $LiMn_2O_4$ electrode exhibits a capacity higher than that of the unmodified $LiMn_2O_4$ electrode (Fig. 4). The difference in the capacity, which appears more remarkably at a high rate of 1.0 C rate, the rate capability of the surface-modified sample was improved rather than in case of the unmodified

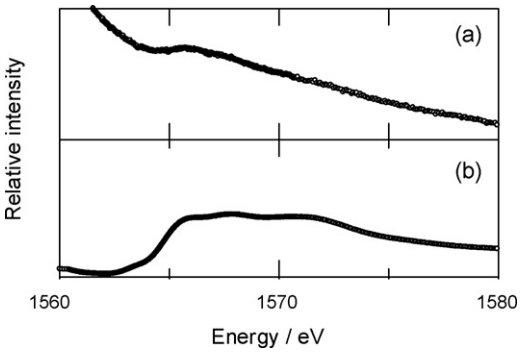

Fig. 2. Al K-edge XANES spectra of (a) Al_2O_3-modified $LiMn_2O_4$ and (b) amorphous Al_2O_3.

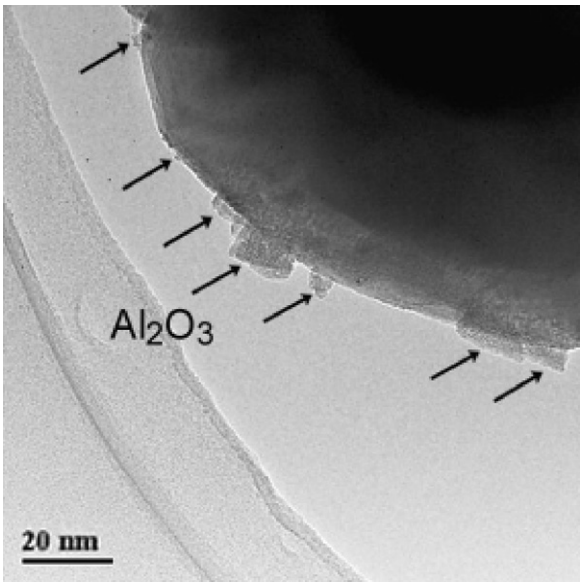

Fig. 3. TEM photograph of Al_2O_3-modified $LiMn_2O_4$ sample.

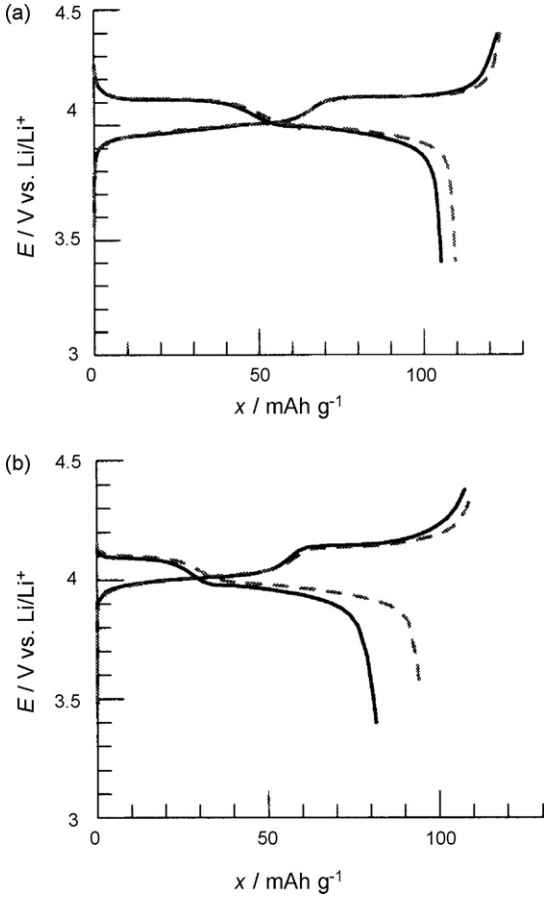

Fig. 4. Charge and discharge profiles of unmodified (full line) and Al_2O_3-modified $LiMn_2O_4$ (dotted line) at (a) 0.1 C and (b) 1.0 C with the cut-off voltages were set at 3.3 V and 4.4 V vs. Li/Li^+. The electrolyte was 1 mol dm^{-3} solution of $LiPF_6$ in 1:1 (vol. ratio) ethylene carbonate (EC)/dimethyl carbonate (DMC).

one. On the other hand, no variation was shown with open circuit potential and apparent chemical diffusion coefficient of Li ion for $LiMn_2O_4$ before and after the surface modification (Fig. 5). The above results explain that the modification of the

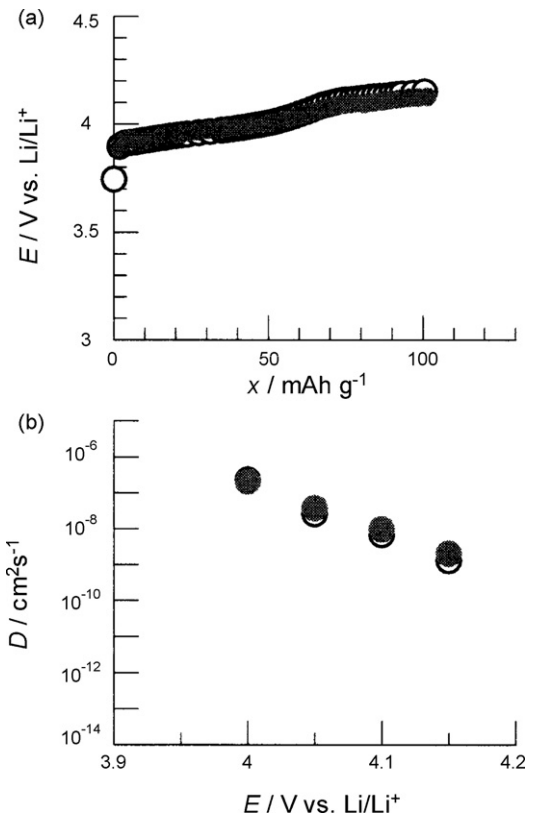

Fig. 5. (a) Open circuit potential for the unmodified $LiMn_2O_4$ (open circle) and Al-modified $LiMn_2O_4$ (solid circle) at room temperature, and (b) the apparent chemical diffusion coefficient of lithium cation insertion calculated from Warburg impedance for the unmodified (full line) and Al_2O_3-modified $LiMn_2O_4$ bulk (dotted line) at room temperature. The electrolyte was 1 mol dm^{-3} solution of $LiPF_6$ in 1:1 (vol. ratio) EC/DMC.

surface promotes the electrochemical reaction on the electrode surface.

To examine the said difference in charge/discharge characteristics between the unmodified and the Al_2O_3-modified $LiMn_2O_4$, electrochemical impedance spectroscopic measurements (EIS) were conducted for both the electrodes at 4.0 V (vs. Li/Li^+) at different temperatures by using various types of lithium salt concentration in the electrolyte. Typical Nyquist plots obtained from the impedance measurements of the unmodified and Al_2O_3-modified $LiMn_2O_4$ consist of two semicircles in the high and medium frequency ranges, and a thin line at a constant angle is inclined to the real axis. Inclination of the line is brought about by the diffusion of the lithium in the $LiMn_2O_4$ bulk [11]. Various types of the models have been proposed with a view to explaining the behavior of the high-frequency semicircles in the Nyquist plots for the insertion electrode [12]. However none of sufficient identification concerning the origin of the high-frequency semicircles has been made up until present. It is generally made known that the medium frequency semicircle is produced by the charge-transfer on the electrode surface [13]. Analysis was made respect to with the impedance spectra using a simple equivalent circuit generally applicable to the lithium transition metal oxide for cathode materials. Fig. 6(a) illustrates the equivalent circuit model used to analyze the obtained impedance spectra. R_s and R_1 represents the electrolyte resistance and the resistance for high frequency. To account for the depression of the high frequency semicircle, a constant phase element (CPE) was introduced in place of capacitor into this model. The CPE is commonly used to describe the

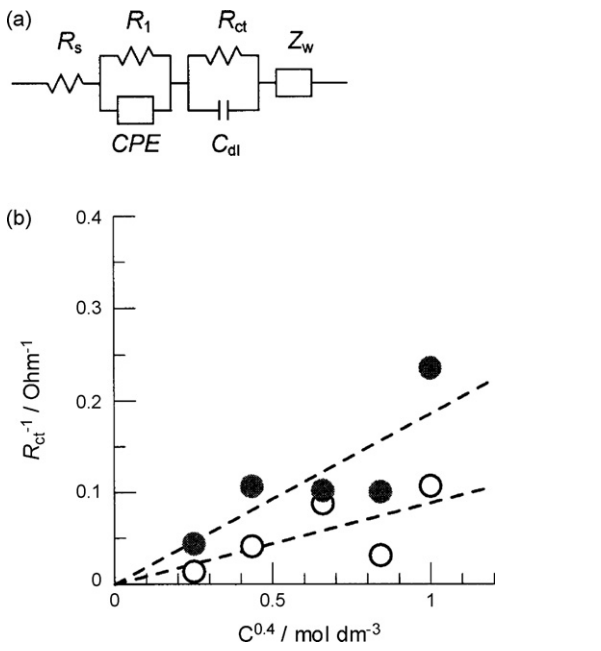

Fig. 6. (a) The equivalent circuit model used to analyze the obtained impedance spectra and (b) plots of inverse R_{ct} vs. lithium salt concentrations in electrolyte for the unmodified $LiMn_2O_4$ (open circle) and Al-modified $LiMn_2O_4$ (solid circle) at room temperature.

depressed semicircle that results from a porous electrode. R_{ct} is the charge-transfer resistance, C_{dl} is the double-layer capacitance, and Z_W is the Warburg impedance. In order to evaluated each kinetics parameters, the non-linear least-squares fitting program was applied within the measured frequency region. The chi-square value of the fit was low, the curve fitting results were good agreement with the actual measurement value. In the meantime, Fig. 6(b) depicts the plots of inverse R_{ct} vs. lithium salt concentrations in electrolyte for the Al-modified and unmodified $LiMn_2O_4$. The result from the above showed the obtained R_{ct} that satisfied the Butler–Volmer equation with all lithium concentrations in the electrode [14]. Between the Al_2O_3-modified $LiMn_2O_4$ and the unmodified one, there is no significance difference in resistance R_1 values for high frequency. However for the medium frequency of the Al_2O_3-modified $LiMn_2O_4$, R_{ct} was smaller than that of the unmodified $LiMn_2O_4$ at all lithium concentration in the electrolyte as shown in Fig. 6(b).

Fig. 7 shows plots of R_{ct} at 4.0 V (vs. Li/Li$^+$) against 10^3 T^{-1} for the unmodified $LiMn_2O_4$ and Al_2O_3-modified $LiMn_2O_4$. From EIS measurements at lower electrolyte concentration, it is explained that difference in R_{ct} is much more in existence before and after the surface modification. From the results of EIS shown in Figs. 6(b) and 7, it is explained that owing to a significant amount of the surface modification, decrease in the charge-transfer resistance on the electrode/electrolyte interface was noted. With the charge-transfer kinetics, improvement was continuously made by surface modification. Therefore it may suggest that the electrochemical potential of lithium cation was increasing on the electrode/electrolyte interface when Al_2O_3 is in existence on the electrode surface. Taking into account Scrosati and co-workers's [8] view, it is imagined that dissociation of lithium cation at electrode/electrolyte interface is facilitated by interaction of counter anions in the electrolyte and aluminum oxide on the electrode surface. Additional work based on EIS, theoretical calculation, and Raman spectroscopy is in progress with a view to providing further support to the counter anions and aluminum oxide interaction model hereby proposed.

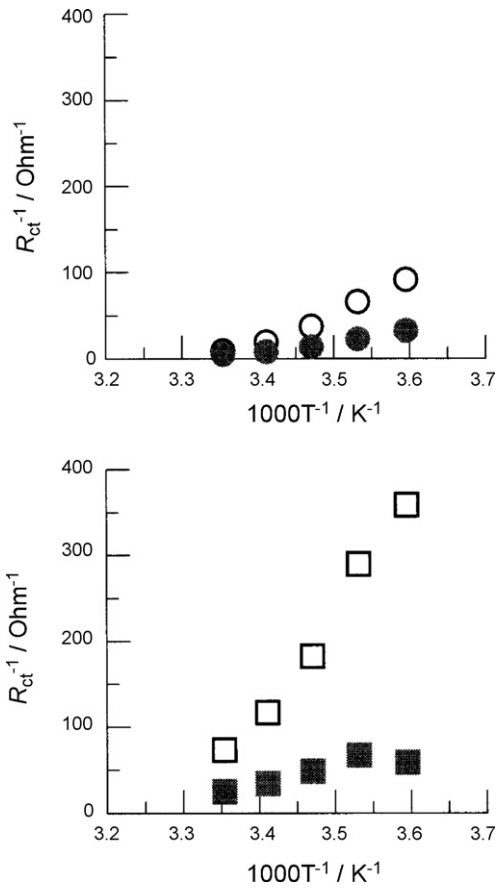

Fig. 7. Plots of R_{ct} at 4.0 V (vs. Li/Li$^+$) against 10^3 T^{-1} for the unmodified $LiMn_2O_4$ (open points) and Al-modified $LiMn_2O_4$ (filled points) in (a) 1 mol dm^{-3} and (b) 0.1 mol dm^{-3} solution of $LiPF_6$ in 1:1 (vol. ratio) EC/DMC.

4. Conclusion

In conclusion, description is herewith made. Modification is made with the spinel $LiMn_2O_4$ electrode surface using Al_2O_3 that plays an important role in increasing the electrochemical potential on the electrode/electrolyte interface. Thus considerable improvement was noticed with the charge-transfer kinetics, electrochemical performance, and importance of interfacial reaction. The results that have obtained to now are quite helpful to the battery industry for affording better understanding of the Li-ion transfer reaction mechanism on the interface than now. Therefore it is desirous to find a solution to this long-pending problem.

References

[1] (a) J.-M. Tarascon, M. Armand, Nature 414 (2001) 359–367;
(b) M. Wakihara, L. Guohua, H. Ikuta, Lithium Ion Batteries, Chapter 2, Kodansha, Tokyo, 1998;
(c) B. Scrosati, Nature 573 (1995) 557–558.
[2] (a) M. Nakayama, H. Ikuta, Y. Uchimoto, M. Wakihara, J. Phys. Chem. B 107 (2003) 10603–10607;
(b) S. Kobayashi, Y. Uchimoto, J. Phys. Chem. B. 109 (2005) 13322–13326.
[3] K. Dokko, M. Mohamedi, M. Umeda, I. Uchida, J. Electrochem. Soc. 150 (2003) A425–A429.
[4] N. Sata, K. Eberman, K. Eberl, J. Maier, Nature 408 (2000) 946–949.
[5] J. Maier, Prog. Solid State Chem. 23 (1995) 171–263.
[6] (a) X. Guo, J. Maier, J. Electrochem. Soc. 148 (2001) E121–E126;
(b) X. Guo, W. Sigle, J. Maier, J. Am. Ceram. Soc. 86 (2003) 77–87.
[7] C.C. Liang, J. Electrochem. Soc. 120 (1973) 1289–1292.
[8] F. Croce, G.B. Appetecchi, L. Persi, B. Scrosati, Nature 394 (1998) 456–458.
[9] (a) J. Cho, Y.J. Kim, T. Kim, B. Park, Angew. Chem. Int. Ed. 40 (2001) 3367–3369;

(b) J. Cho, Y.W. Kim, B. Kim, J.G. Lee, B. Park, Angew. Chem. Int. Ed. 42 (2003) 1618–1621.
[10] K. Shimizu, Y. Kato, T. Yoshida, H. Yoshida, A. Satsuma, T. Hattori, Chem. Commun. (1999) 1681–1682.
[11] C. Ho, I.D. Raistrick, R.A. Huggins, J. Electrochem. Soc. 127 (1999) 343–350.
[12] (a) D.M. Levi, G. Salitra, B. Markovsky, H. Teller, D. Aurbach, U. Heider, J. Electrochem. Soc 146 (1999) 1279–1289;
(b) K. Dokko, M. Mohamedi, Y. Fujita, T. Itoh, M. Nishizawa, M. Umeda, I. Uchida, J. Electrochem. Soc. 148 (2001) A422–A426;
(c) F. Nobili, R. Tossici, R. Marassi, J. Phys. Chem. B 106 (2002) 3909–3915;
(d) Y.-M. Choi, S.-I. Pyun, J.-S. Bae, S.-I. Moon, J. Power Sources 56 (1995) 25–30;
(e) A.-K. Hjelm, G. Lindbergh, Electrochem. Acta. 47 (2002) 1747–1759.
[13] D. Aurbach, M.D. Levi, H. Teller, B. Markovsky, G. Salitra, J. Electrochem. Soc. 145 (1998) 3024–3034.
[14] A.J. Bard, L.R. Faulkner, Electrochemcal Methods. Fundamentals and Applications, 2nd ed., John Wiley & Sons, New York, 2001, Chapter 3.